Journal of Materials Chemistry B

Accepted Manuscript

ROYAL SOCIETY OF CHEMISTRY

www.rsc.org/materialsB

Cite this: DOI: 10.1039/c0xx00000x

www.rsc.org/xxxxxx

ARTICLE TYPE

Three label-free thrombin aptasensors based on aptamers and $[Ru(bpy)_2(o\text{-}mopip)]^{2+}$

Juanjuan Li, Xiaochun Hu, Shuo Shi*, Yiwei Zhang and Tianming Yao*

Received (in XXX, XXX) Xth XXXXXXXXX 20XX, Accepted Xth XXXXXXXXX 20XX
DOI: 10.1039/b000000x

Early diseases diagnosis is very important for the prevention or mitigation of metastasis. Effective and efficient methods are needed to improve the diagnosis and assessment of diseases. Thrombin is a biomarker for diagnosis of some diseases, such as pulmonary metastases and diseases associated with coagulation abnormalities. Lots of methods for detecting thrombin have been reported, however, most of them were based on a single aptamer and needed modification of aptamer, label free sensors for thrombin detection based on aptamer pair are challenging. In this work, we present three label free sensing platforms based on $[Ru(bpy)_2(o\text{-}mopip)]^{2+}$ (bpy=2,2-bipyridine; o-mopip=2-(2-methoxylphenyl) imidazo [4,5-f][1,10] phenanthroline) (OMO) and graphene oxide (GO) for thrombin detection. Our three label free detection is accomplished by specific target recognition based on aptamer pair TBA1/TBA2-thrombin, single aptamer TBA1-thrombin or TBA2-thrombin, respectively. Direct readouts of the target recognition is achieved by restoration of the fluorescence of OMO prequenched by GO. All of the three sensing platforms exhibited high sensitivity and selectivity. Furthermore, all sensing platforms were successfully applied to thrombin analysis in diluted bovine serum. According to thrombin dependent response of the three platforms, the sensing platform based on aptamer pair TBA1 and TBA2 showed highest sensitivity, widest linearity, best selectivity and recovery in diluted serum to thrombin. These results show that the sensing platform based on aptamer pair have great promise for clinical diagnosis of disease-related biomarkers.

1. Introduction

Current cancer diagnostics mainly rely on commercialized multistep antibody based binding assays, such as, ELISA (enzyme-linked immunosorbent assay), luminex, and nanosphere for capturing and monitoring target proteins.[1] However, the antibody-based methods require large sample volumes, expensive reagents, or a multistep assay with associated long incubation times. Furthermore, antibody affinity varies from batch to batch, which makes it difficult to develop reliable sensors for clinical molecular diagnostics.

Aptamers are RNA or single stranded DNA molecules that selectively bind to various molecular targets.[2] They bind to molecular targets with high specificity and affinity, making them attractive alternatives to the commonly used antibodies.[3] Aptamers for specific targets can be artificially isolated from combinatorial libraries of oligomers via systematic evolution of ligands by exponential enrichment (SELEX) technique.[4] It has been demonstrated that some proteins even have two aptamers that can selectively bind to specific and different epitopes of them, such as, thrombin, vascular endothelial growth factor165, platelet-derived growth factor and so on. In particular, the thrombin binding aptamer 1 (TBA1) and 2 (TBA2) consist of two G-quadruplex conformations that selectively bind to specific and different epitopes of thrombin.[5] TBA1 is a 15-mer DNA aptamer which binds exosite I of thrombin (Fibrinogen binding site) with nanomolar affinity, while TBA2 is a 29-mer DNA aptamer binding to exosite II of thrombin (Heparin binding domain) with subnanomolar affinity.[5]

Thrombin is the main effector protease of the coagulation cascade, which converts circulating fibrinogen to fibrin monomer, and then polymerizes to form fibrin, the fibrous matrix of blood clots.[6] What's more, thrombin also can act as a hormone to regulate platelet aggregation, endothelial cell activation, and other important responses in vascular biology.[6] Most importantly, thrombin can be used as a therapeutic and a biomarker for diagnosis of some diseases, such as pulmonary metastases and diseases associated with coagulation abnormalities.[7] Under normal conditions, the concentration of thrombin in blood varies from nanomolar to low micromolar levels during the coagulation progress.[7] Therefore, it is important for clinical diagnosis to detect thrombin level.

Recently, various aptasensors have been reported for the detection of thrombin by using different signal readout assays including electrochemiluminescence,[8, 9] electrochemistry,[10-14] colorimetry,[7, 15] surface plasmon resonance,[16] surface enhanced

raman scattering,[17] fluorescence resonance energy transfer (FRET),[18, 19] resonance light scattering,[2] and so on. Sensors for thrombin detection were mostly based on a single aptamer, and only a few articles have been reported to detect thrombin based on two aptamers. A previously reported microarray sensor to detect thrombin based on two aptamers,[5] however, this method needed modifications of the aptamer. Another sandwich aptamer microarray sensor for thrombin detection with the need of protein labeling and modifications of the aptamer.[20] These methods are limited by either the sensor size or sensitivity or by the associated assay complexity. For example, electrochemical sensors designed to measure an electron transfer require electrodes on a millimeter scale to achieve sufficient sensitivity and colorimetric require collecting a large amount of particles to induce a discernible color change.[1] And most reported FRET aptasensors require dual-label modifications of the aptamer probes with fluorophores and quenchers (or fluorophore donors and acceptors), which is laborious, time-consuming and expensive. Furthermore, dual labeling of aptamers can often weaken the binding affinities between aptamers and the corresponding targets and influence the sensitivity for detection,[21] which limited their extended applications. Until now, label free aptasensor for thrombin detection has rarely been reported and we supposed that maybe label free aptasensor based on aptamer pair is better than aptasensor based on single aptamer.

Herein, in order to demonstrate this hypothesis, we present three label-free aptasensors based on FRET by combining aptamer-target interaction for target recognition and graphene oxide-$[Ru(bpy)_2(o\text{-}mopip)]^{2+}$ (bpy=2,2-bipyridine; o-mopip=2-(2-methoxylphenyl) imidazo[4,5-f][1,10] phenanthroline) (OMO) interaction for signal readouts. And the study shows that the aptasensor based on aptamer pair showed a higher sensitivity, a wider linearity, better selectivity and recovery in diluted serum to thrombin than aptasensor based on single aptamer. The developed aptasensors are simple, sensitive, specific and stable for the detection of thrombin.

2. Experimental section

2.1 Materials and methods

DNA sequences used in this work are listed as follows. The sequence of TBA1 was: 5'-GGT TGG TGT GGT TGG-3'. The sequence of TBA2 was: 5'-AGT CCG TGG TAG GGC AGG TTG GGG TGA CT-3'. All of the synthesized oligonucleotides were purchased from Shanghai Sangon Biotechnology Co. Ltd. (Shanghai, China). Thrombin was purchased from Sigma-Aldrich (St. Louis, MO, USA), dissolved in deionized purified (MilliQ) water, aliquoted and stored as recommended by the supplier. OMO was synthesised by our group (The synthesized method and characterization of OMO were provided in the supporting information). All the other chemicals were at least of analytical reagent grade, purchased from Aladdin Ltd. (Shanghai, China) and Sinopharm Chemical Reagent Co. Ltd. (Shanghai, China), and used directly without further purification.

Fluorescence spectra were recorded at room temperature via an F-7000 fluorescence spectrophotometer (Hitachi Ltd., Japan) in a 1.0 cm path length quartz cuvette. The slot widths for both excitation and emission were fixed at 10 nm. The excitation wavelength was λ = 460 nm. The transmission electron microscopies were recorded on a high-resolution transmission electron microscope (Tecnai G^2 F20 S-Twin). Atomic force microscope (AFM) (Bruker Multimode 8) was used to characterize the thickness of the samples in the peakforce mode. The composition information was conducted by energy dispersive X-ray spectroscopy (EDS) at 20 keV on a X-Max T80 EDS instrument (oxiford). Circular dichroism (CD) spectra were measured on a Jasco J-815 spectropolarimeter, with a scanning speed of 100 nm/min and the response time was set to 0.25 s (A quartz cuvette with 1.0 cm path length was used for all spectra scanning samples).

2.2 Preparation of aptamers-thrombin complex

The aptamers of thrombin were dissolved in 10 mM Tris-HCl, 1 mM EDTA, 100 mM KCl, pH = 8.0. Prior to incubation with their targets, all the aptamer samples were denatured at 95 °C for 5 minutes and the samples were left to cool to room temperature (slow annealing). Thrombin with the increasing concentration (from 0 to 1225.0 nM) and 10 μL (5 μM) annealed TBA1 or/and TBA2 were mixed in binding buffer (10 mM Tris-HCl, 100 mM NaCl, 0.05 mM EDTA, pH = 7.4) in a total volume of 210 μL, incubated at 25 °C for 40 min.

2.3 Construction of GO-OMO-aptamers-thrombin complex

10 μL (200 μM) OMO were added into each aptamers-thrombin sandwich complex sample and incubated for one hour at room temperature. After that, 40 μL (200 ug/ml) GO were added to each sample, which was diluted to 1 mL by working buffer (10 mM Tris-HCl, pH = 7.0), and incubated at room temperature for another hour. The final concentration of GO, TBA1/TBA2 and OMO were 8 μg/ml, 0.05 μM and 2 μM, respectively.

3. Results and discussion

3.1 Characterization of graphene oxide (GO) and GO-OMO hybrid

The samples used for AFM studies were prepared by depositing the corresponding dispersions on new cleaved mica surfaces and dried at room temperature. As shown in Fig. S1, the average vertical distance of monolayer GO and GO-OMO were 1.02 nm and 1.44 nm, respectively, indicating that the surface of GO was covered with OMO. High resolution transmission electron microscopy (TEM) was further used to characterize the morphology of GO and GO-OMO hybrid (Fig. S2.) It was noted that the GO surface was rough with a significant number of wrinkles. However, the surface of GO-OMO hybrid became more smooth, due to homogeneous adsorption of OMO on the surface of GO, which was consistent with the previous reports.[23] In addition, the EDS analysis of GO-OMO hybrid showed C/O with an amount of Ru (Fig. S3B), which illustrated that the as-obtained products consist of GO and Ru.

3.2 Thrombin detection strategy

OMO shows strong fluorescence in Tris-HCl buffer (pH = 7.0) at room temperature, its metal-to-ligand charge transfer (MLCT) transition can be perturbed with binding to DNA, providing a

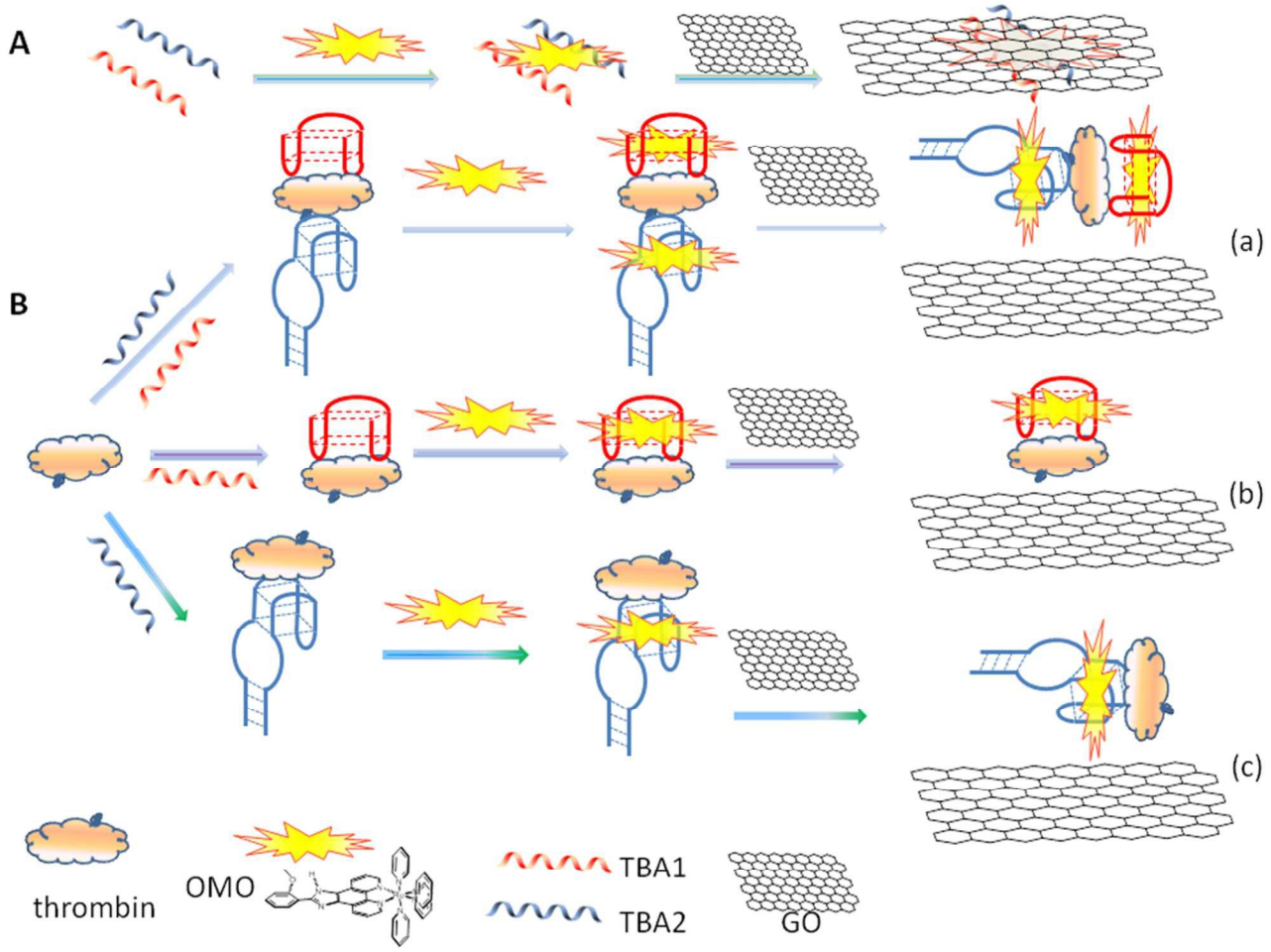

Scheme. 1 Schematic depiction of the aptamers-GO-OMO biosensor based on FRET for detection of thrombin. (A) OMO can bind to TBA1 and TBA2, providing a remarkable enhancement in the luminescence, and the fluorescence can be quenched by GO. (B) (a) Detect thrombin based on aptamer pair: In the presence of thrombin, TBA1 and TBA2 folded into G-quadruplex. OMO bound with the newly formed G-quadruplex, dissociated from the surface of GO with G-quadruplex.(b) Detect thrombin based on single aptamer TBA1.(c) Detect thrombin based on single aptamer TBA2.

remarkable enhancement in the luminescence.[22] Graphene oxide is a good energy acceptor in energy transfer, it can act as a quencher to quench the fluorescence of Ru complex via π-π interactions and electrostatic interactions.[23] In addition, GO can differentiate various DNA structures such as single-stranded DNA (ssDNA), double-stranded DNA (dsDNA), stem-loops and G-quadruplex due to their characteristic interactions with GO. SSDNA (aptamer) can be adsorbed on the surface of GO via π-π interaction. However, G-quadruplex structure cannot be absorbed by GO.[24] An illustration of aptamers-GO-OMO biosensor based on FRET to detect thrombin is shown in scheme 1. (A) OMO can bind with TBA1 and TBA2, providing a remarkable enhancement in the luminescence, however, when GO was added, both OMO and single DNA aptamers were absorbed by GO, resulting in the florescence of OMO being quenched. (B) In the presence of thrombin, TBA1 and TBA2 selectively bind to specific and different epitopes of thrombin,[5] folding into G-quadruplex.[5]. Then, OMO bound with the newly formed G-quadruplex probably by π-π stacking just like $[Ru(bpy)_2(pip)]^{2+}$ (bpy = 2,2'-bipyridine; pip = 2-phenylimidazo[4,5-f][1,10] phenanthroline),[24] disturbing the interaction between OMO and GO, OMO with G-quadruplex dissociated from the surface of GO, resulting in the restoration of florescence.

3.3 Feasibility of strategy

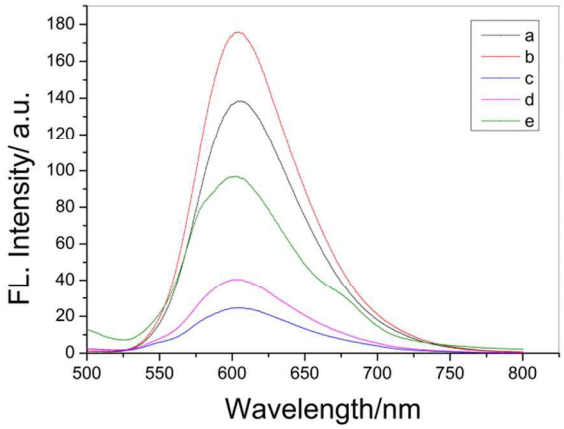

Fig. 1 Fluorescence emission spectra of OMO (a), OMO+ aptamers (b), OMO+GO (c), OMO+ GO+ aptamers (d), OMO+ GO+ aptamers+thrombin (e).The concentrations of TBA1, TBA2, thrombin, OMO and GO were 50, 50, 123, 2000 nM and 8 μg/mL, respectively.

The feasibility of the proposed method was demonstrated by fluorescence emission spectra of OMO under different conditions (Fig. 1). OMO exhibited strong fluorescence intensity (curve a). that was quenched by GO (curve c) via π-π interactions and electrostatic interactions.[23] OMO-aptamer pair complex exhibited stronger fluorescence (curve b) owning to that OMO intercalated DNA, providing a remarkable enhancement in the luminescence.[22] However, the fluorescence spectrum of GO-aptamers-OMO exhibited extremely weak fluorescence (curve d) owing to that TBA1, TBA2 (ssDNA) and OMO were absorbed on GO surface. The introduction of thrombin brought about big change of fluorescence intensity (curve e), owning to that OMO bound with the newly formed G-quadruplex, and dissociated from the GO surface with G-quadruplex. The results indentified that thrombin triggered the fluorescence recovery of OMO, leading to a "signal-on" fluorescence of sensing platform.

To further clarify G-quadruplexes conformations in the presence of thrombin, circular dichroism (CD) spectroscopy measurements were carried out. As shown in Fig S4A, CD spectra of TBA1 alone at room temperature exhibited a negative band centered at 265 nm, as well as a major positive band at 295 nm. Upon the addition of thrombin, the negative band at 265 nm decreased, and the positive band at 295 nm increased, indicating the formation of chair-like intramolecular anti-parallel G-quadruplex structure, which was consistent with the previous reports.[25] Similarly, thrombin can promote TAB2 to form anti-parallel G-quadruplex too.[26] The CD spectra of the mixture of TBA1 and TBA2 at room temperature exhibited a negative band centered at 235 nm and a major positive band at 295 nm (Fig S4B), which probably corresponded to the signal of the random-coil aptamers (characterized by a negative peak at 235 nm) and anti-parallel G-quadruplex (characterized by a positive peak at 295 nm), respectively. In the presence of thrombin, the weak negative bands around 235 nm disappeared and the positive band at 295 nm increased, indicating that the random-coil was transformed into the anti-parallel G-quadruplex by thrombin. These changes in the CD spectrum of aptamers after the addition of thrombin were consistent with fluorescence emission spectra.

3.4 Optimization of conditions

In order to achieve the optimal performance, the concentration of GO as a critical factor for detection efficiency was optimized. As shown in Fig. 2A, the fluorescence intensity decreased as the concentration of GO increased. When the concentration of GO was added to 8 ug/ml, the florescence of OMO was quenched by 85%, after that, there was no significantly decrease of florescence with more GO (Fig. 2B). What's more, extra GO is adverse to the restoration of fluorescence. Therefore, the corresponding concentration of GO (8 μg /mL) was chosen as the optimal value for the next experiments to detect thrombin.

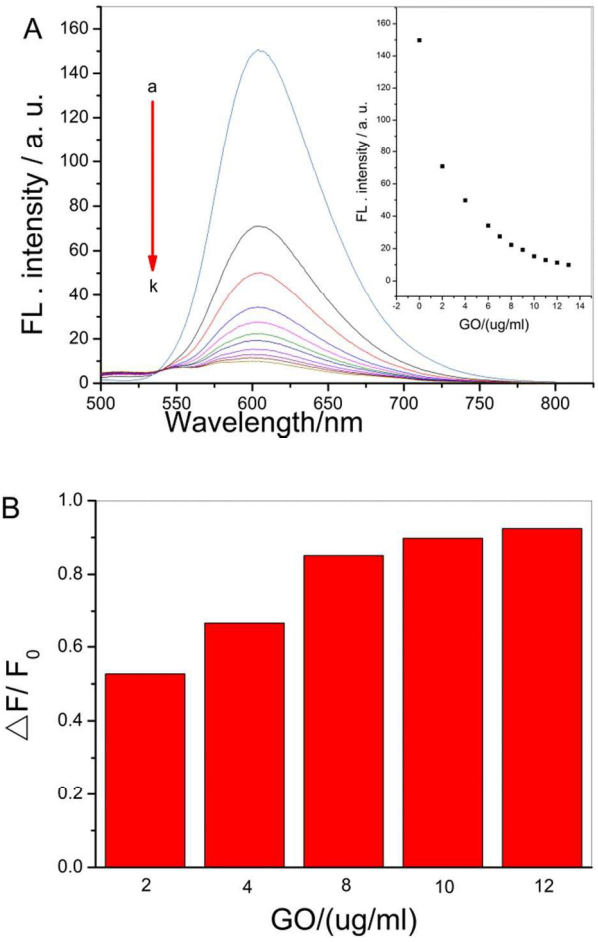

Fig. 2 (A) Effects of GO concentration on the fluorescence intensity. Fluorescence emission spectra of sensing platform in response of GO at 0, 2, 4, 6, 7, 8, 9, 10, 11, 12 and13 μg/ml (form a to k). (B) Effects of GO concentration on the quenching efficiency. ΔF is the fluorescent difference of sensing system in the absence and presence of GO. All assays were carried out in 10 mM Tris-HCl, pH = 7.0 with the concentrations of TBA1, TBA2 and OMO were 0.05, 0.05 and 2 μM, respectively.

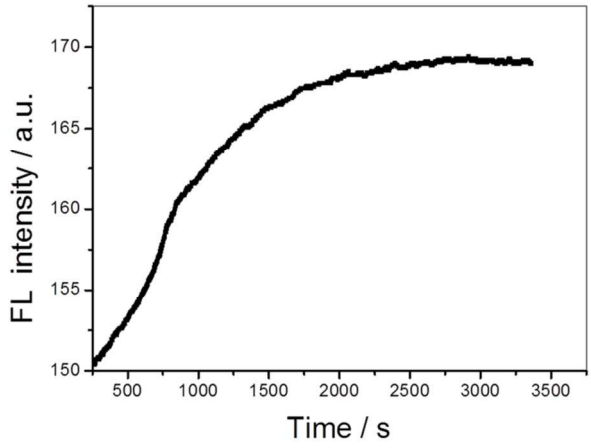

Fig. 3 Effect of incubation time of aptamers-thrombin-OMO on the fluorescence intensity before GO was added. The concentration of TBA1, TBA2 and thrombin were 50, 50, and 47.5 nM, respectively.

The fluorescent difference of GO-OMO-aptamers with/without thrombin is important for detection efficiency. Thus, it is important to gain the highest fluorescence intensity of aptamers-thrombin-OMO complex before GO was added. In order to achieve the above objective, the incubation time of aptamers-thrombin-OMO was optimized. As shown in Fig. 3, the fluorescence of the complex increased quickly during 0-900 seconds, and increased slowly during 900 to 1500 seconds. There was almost no change of fluorescence intensity when the complex was incubated more than 2800 seconds, meaning the equilibrium of the reaction system. Therefore, one hour is enough to gain the highest fluorescence intensity of aptamers-thrombin-OMO complex.

3.5 Analytical application in determination of thrombin

To measure thrombin concentration-dependent response of this platform, various concentrations of thrombin from 3.7 to 1225.0 nM were incubated with OMO-aptamer pair-GO complex. Fig. 4 shows the differential fluorescence intensity of the aptasensor in different concentrations of thrombin under optimal experimental conditions. The fluorescence intensity increased with thrombin concentration. The more thrombin was added, the more G-quadruplex was formed, resulting in more OMO dissociating from GO with the newly formed G-quadruplex. As a result, the higher fluorescence intensity was observed. A linear relationship between the fluorescence intensity and thrombin concentration was obtained covering the concentration range from 3.7 to 612.7 nM (R^2 = 0.991) with a detection limit of 0.76 nM (defined as 3S/slope, where S is the relative standard deviation of a blank solution, n = 11).

For comparison, label-free aptasensor based on single aptamer TBA1 or TBA2 were carried out. The thrombin aptamer TBA1 or TBA2 forms a G-quadruplex upon its association to the protein. This allows OMO to bind with the newly formed G-

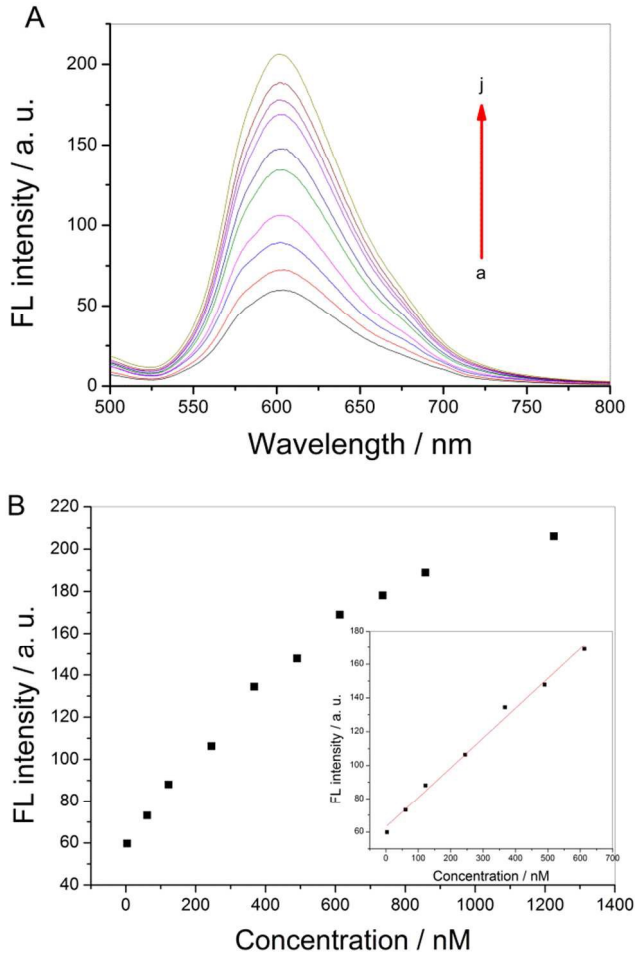

Fig. 4 (A) Fluorescence emission spectra of sensing platform in response of thrombin at 3.7, 61.25, 122.5, 245.0, 367.6, 490.2, 612.7, 735.3, 857.9, and 1225.0 nM (from a to j). (B) Calibration curve for thrombin detection.

Table 1 Comparison of the proposed work with other methods for thrombin determination

Method	Linear calibration range (nM)	Detection limit (nM)
A sensor based on surface plasmon resonance[6]	0.1-75	0.1
A aptasensor based on SYBR Green I dye[21]	0-500	1.1
A fluorescence sensor based on split aptamer fragments[27]	0-20	2
Fluorescent detection based on H_2O_2-catalyzed oxidation via hemin /G-quadruplex DNAzyme[28]	0-100	10
Fluorescent detection based on inhibition of polymerase reaction[29]	0-500	62.5
Aptamer-functionalized Au nano-particles for the amplified optical detection of thrombin[30]	0-120	20
This work based on aptamer pair (TBA1 and TBA2)	3.7 to-613	0.76
This work based on aptamer TBA1	33.9- 407.0	1.12
This work based on aptamer TBA2	33.9- 407.0	0.92

quadruplex and the subsequent generation of fluorescence as a readout signal. As shown in supporting information (Fig. S5 and Fig. S6), the method based on single aptamer enabled the analysis of thrombin with a detection limit of 1.12 and 0.92 nM, respectively, covering the concentration range from 33.9 to 407.0 nM.

In conclusion, the study shows that the aptasensor based on aptamer pair has better linear range and detection limit for thrombin than that based on single aptamer. The linear range and detection limit of this imprinted sensor based on aptamer pair for thrombin determination are much better than other methods,[6,21,27,28,29,30] details are given in table 1.

3.6 Interference and Selectivity

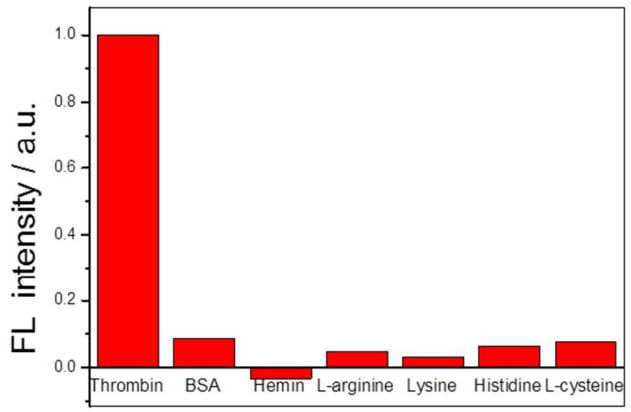

Fig. 5 Fluorescence intensity changes of the aptasensor toward thrombin and other biomoleculars under the same condition. The concentrations of thrombin, hemin, BSA, L-arginne, histidine and L-cysteine were 556 nM, respectively.

To evaluate the selectivity of our strategy for thrombin, the fluorescence responses of sensing platform to thrombin and other biomolecules, including BSA, hemin, L-arginine, lysine, histidine and L-cysteine were individually investigated at the same concentration. As shown in Fig. 5 (aptasensor based on aptamer pair TBA1 and TBA2), Fig. S7 and Fig. S8 (aptasensor based on single aptamer, for detailed information see the supporting information), the fluorescence intensity of thrombin were about 10 times, 9 times and 9 times higher than that of BSA, hemin, L-arginine, lysine, histidine and L-cysteine, respectively. These results indicated the good selectivity and high specificity of the three proposed aptasensors to thrombin, which was attributed to the high selectivity of aptamers to its target. In addition, these results indicated that the selectivity of aptasensor based on aptamer pair was better than aptasensor based on single aptamer, probably because that TBA1 and TBA2 cooperated with each other to detect thrombin.

3.7 Detection in serum

Table 2 Detection of thrombin in diluted serum samples. (N=3)

Samples	Amount spiked (nM)	Amount measured(nM)	Recovery (%)	RSD (%)
1	130	140.07	107.7	0.93
2	260	281.32	108.2	1.1
3	520	544.46	104.7	0.74

To demonstrate the application of these constructed aptasensors to real life samples, several samples were prepared by spiking different amounts of thrombin into serum samples that has been diluted 500 times by PBS (10 mM pH = 6.5) buffer to minimize nonspecific adsorption. The detection results for above prepared samples are presented in Table 2 (based on aptamer pair), Table S1 and Table S2 (based on single aptamer), respectively. The recoveries were 104.7 % - 108.2 %, 90.6 % - 118.0 % and 85.9 % - 92.8 %, respectively. And relative standard deviation (RSD) were 0.74 % - 1.1 %, 0.78 % - 1.5 % and 0.98% - 1.4 %, respectively. These results indicated that these proposed FRET aptasensors had promising sensing abilities even in complex biological samples and the recovery of thrombin based on aptamer pair was better than that of single aptamer.

4. Conclusions

In summary, we have demonstrated three label free biosensors for thrombin detection based on TBA1, TBA2 and OMO. Under the optimized experimental conditions, the aptasensor based on aptamer pair showed a higher sensitivity, wider linearity, better selectivity and recovery in diluted serum to thrombin than aptasensor based on single aptamer TBA1 or TBA2. These aptasensors provided high specificity for thrombin against BSA, hemin, L-arginine, lysine, histidine and L-cysteine, and were successfully applied to thrombin analysis in diluted bovine serum, exhibiting great opportunities for practical application in biological and clinical diagnosis fields. Compared with other assays for thrombin, this study is meaningful for several reasons: Firstly, our sensors did not need modifications of the aptamer probes with fluorophores and quenchers (or fluorophore donors and acceptors) which is simple, fast, sensitive and cost-effective. Secondly, this study built up a new method for aptamer-based sandwich assay to detect protein. This strategy had the potential for development of assays for other targets with excellent performance.

Acknowledgements

This work was supported by the National Natural Science Foundation of China (31170776, 81171646, and 21472139), the Fundamental Research Funds for the Central Universities and the Science and Technology Commission of Shanghai Municipality (14DZ2261100).

Notes and references

Shanghai Key Lab of Chemical Assessment and Sustainability, Department of Chemistry, Tongji University Shanghai, 200092 (P.R. China)；
Tel: +86 65983292
Fax: +86 65982287
**E-mail: shishuo@tongji.edu.cn tmyao@tongji.edu.cn*

1 H. Cho, E.-C. Yeh, R. Sinha, T. A. Laurence, J. P. Bearinger and L. P.Lee, *ACS Nano*, 2012, **6**, 7607-7614.
2 X. P. Huang, Y. Q. Li, X. Huang, Y. W. Chen and W. H. Gao, *Rsc Advances*, 2015, **5**, 30268-30274.
3 W. Bai, N. A. Gariano and D. A. Spivak, *J. Am. Chem. Soc.*, 2013, **135**, 6977-6984.
4 S. M. Taghdisi, N. M. Danesh, P. Lavaee, A. S. Emrani, M. Ramezani and K. Abnous, *Rsc Advances*, 2015, **5**, 43508-43514.
5 A. Meneghello, A. Sosic, A. Antognoli, E. Cretaio and B. Gatto, *Microarrays*, 2012, **1**, 95-106.
6 Y. Bai, F. Feng, L. Zhao, C. Wang, H. Wang, M. Tian, J. Qin, Y. Duan and X. He, *Biosens. Bioelectron.*, 2013, **47**, 265-270.
7 Z. Chen, Y. Tan, C. Zhang, L. Yin, H. Ma, N. Ye, H. Qiang and Y. Lin, *Biosens. Bioelectron.*, 2014, **56**, 46-50.
8 Y. Guo, X. Jia and S. Zhang, *Chem. Commun.*, 2011, **47**, 725-727.
9 X. Y. Wang, A. Gao, C. C. Lu, X. W. He and X. B. Yin, *Biosens. Bioelectron.*, 2013, **48**, 120-125.
10 Y. Y. Chang, S. B. Xie, Y. Q. Chai, Y. L. Yuan and R. Yuan, *Chem. Commun.*, 2015, **51**, 7657-7660.
11 D. Choi, H. Jeong and K. Kim, *Analyst*, 2014, **139**, 1331-1333.
12 J. Hu, T. Wang, J. Kim, C. Shannon and C. J. Easley, *J. Am. Chem. Soc.*, 2012, **134**, 7066-7072.
13 L. P. Xu, S. Wang, H. Dong, G. Liu, Y. Wen, S. Wang and X. Zhang, *Nanoscale*, 2012, **4**, 3786-3790.
14 C. He, Z. Xu, T. Sun and L. Wang, *Appl. Biochem. Biotechnol.*, 2014, **172**, 1018-1026.
15 Y. Niu, P. Wang, Y. Zhao and A. Fan, *Analyst*, 2013, **138**, 1475-1482.
16 P. He, L. Liu, W. Qiao and S. Zhang, *Chem. Commun.*, 2014, **50**, 1481-1484.
17 Z. Wu, Y. Liu, X. Zhou, A. Shen and J. Hu, *Biosens. Bioelectron.*, 2013, **44**, 10-15.
18 X. Q. Liu, F. Wang, R. Aizen, O. Yehezkeli and I. Willner, *J. Am. Chem. Soc.*, 2013, **135**, 11832-11839.
19 F. Luo, L. Y. Zheng, S. S. Chen, Q. H. Cai, Z. Y. Lin, B. Qiu and G. N. Chen, *Chem. Commun.*, 2012, **48**, 6387-6389.
20 A. Sosic, A. Meneghello, E. Cretaio and B. Gatto, *Sensors*, 2011, **11**, 9426-9441.
21 L. Kong, J. Xu, Y. Xu, Y. Xiang, R. Yuan and Y. Chai, *Biosens. Bioelectron.*, 2013, **42**, 193-197.
22 S. Shi, J. Liu, J. Li, K. C. Zheng, X. M. Huang, C. P. Tan, L. M. Chen and L. N. Ji, *J. Inorg. Biochem.*, 2006, **100**, 385-395.
23 L. Wang, T. Yao, S. Shi, Y. Cao and W. Sun, *Sci. Rep.*, 2014, **4**, 5320.
24 W. Sun, S. Shi and T. Yao, *Anal. Methods*, 2011, **3**, 2472.
25 D. Zhao, X. Dong, N. Jiang, D. Zhang, and C. Liu, *Nucleic Acids Res.,* 2014, **42**, 11612-11621.
26 H. Li, W. Li, Z. Nie, and S. Yao, *Analyst*, 2015, **140**, 6386–6391.
27 X. Liu, L. Shi, X. Hua, Y. Huang, S. Su, Q. Fan, L. Wang and W. Huang, *ACS Appl. Mater. Interfaces*, 2014, **6**, 3406-3412.
28 E. Golub, R. Freeman, A. Niazov and I. Willner, *Analyst*, 2011, **136**, 4397-4401.
29 C. Zhu, Y. Wen, D. Li, L. Wang, S. Song, C. Fan and I. Willner, *Chem. Eur. J.*, 2009, **15**, 11898-11903.
30 V. Pavlov, Y. Xiao, B. Shlyahovsky and I. Willner, *J. Am. Chem. Soc.*, 2004, **126**, 11768-11769.

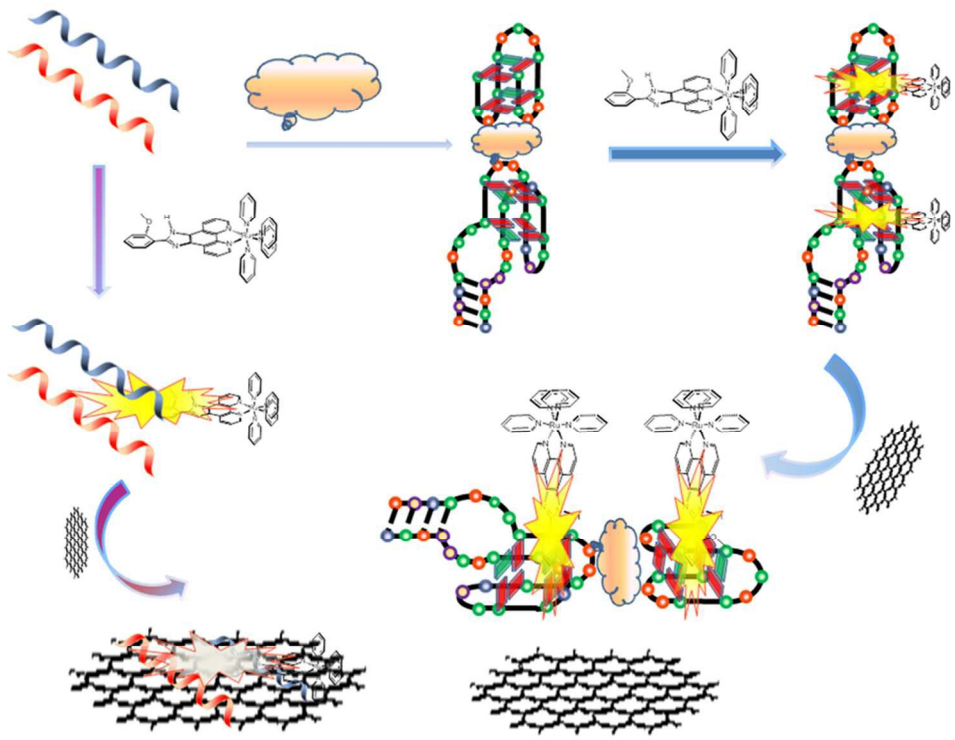

The lable free aptasensor based on aptamer pair and [Ru(bpy)2(o-mopip)]2+-GO has been successfully applied to sandwich assay for thrombin detection.
40x30mm (600 x 600 DPI)